Activation of microglia in the nucleus of the solitary tract by inferior alveolar nerve injury

Rina Kakihara[1], Takeshi Suwabe[4], Yasuo Nishikawa[3] and Shosuke Morita[2]

[1]*Graduate School of Dentistry (First Department of Oral and Maxillofacial Surgery)*, [2]*First Department of Oral and Maxillofacial Surgery*,
[3]*Department of Physiology, Osaka Dental University, 8-1 Kuzuhahanazono-cho, Hirakata-shi, Osaka 573-1121, Japan, and*
[4]*Department Oral Physiology, Oral Functional Science and Rehabilitation, School of Dentistry, Asahi University, 1851 Hozumi, Mizuho-shi, Gifu 501-0296, Japan*

Deafferentation of somatosensory trigeminal nerves innervating dental pulp and periodontal tissue results in a higher taste threshold persisting for a long time in humans. The dental and taste nerves converge on neurons in the rostral nucleus of the solitary tract (rNST), suggesting somatosensory and taste input interact in processing taste information in the rNST. Peripheral injury to the inferior alveolar nerve (IAN), one of the dental nerves, leads to glial responses predominantly in the trigeminal spinal subnucleus caudalis and spinal dorsal horn, and abnormal pain sensation via a mechanism involving the active microglia. We examined the microglial response in another primary IAN terminal, the NST, after transection of the IAN (IANx) to reveal a mechanism of abnormal taste sensation after peripheral injury to the dental nerves. By 7 days post-IANx, a cluster of microglial cells appeared in and around the rostral-most portion of the NST, indicating that nerve damage to the IAN results in a microglial response in the rNST, which may participate in initiating abnormal taste sensations following IAN injury. (J Osaka Dent Univ 2015 ; 49(1) : 21–26)

Key words : Microglia ; Nucleus of solitary tract (NST) ; Inferior alveolar nerve (IAN)

INTRODUCTION

There are reports on hypoesthesia and anesthesia in taste sensation persisting for several months or even years after dental anesthesia, pulpectomy and tooth extraction. Taste disorders following dental treatments are usually attributed to peripheral injury of taste (the chorda tympani) nerve fibers running with the lingual nerve fibers near the mandibular molars.[1, 2] However, taste impairment in patients who received treatment of the maxillary anterior teeth cannot be explained by peripheral nerve injury, because the chorda tympani nerve fibers neither innervate nor run through the anterior surgical site.[3]

The inferior alveolar nerve, a branch of the trigeminal nerve, innervates dental pulp and periodontal tissue. Peripheral fibers of the inferior alveolar nerve are injured upon dental treatments such as pulpectomy and tooth extraction. In particular, there is a risk that the nerve trunk is crushed or torn upon extraction of

mandibular third molars, because the IAN runs in the mandibular canal in close proximity to the molar root tips. Following peripheral nerve injury, glial cells respond at the primary nerve terminals in the central nervous system. In animal models of inferior alveolar nerve injury, microglia appear in the trigeminal spinal subnucleus caudalis and spinal dorsal horn[4] and release substances that affect neuronal excitability.[5–7] Inhibition of microglial activation suppresses development of pain hypersensitivity,[4] suggesting that active microglia cause abnormal pain sensation by alteration of excitability in neurons processing somatosensory information. The inferior alveolar nerve also terminates in synapses with neurons of the rostral nucleus of the solitary tract where taste afferents terminate.[8] In light of these observations, inferior alveolar nerve injury may activate microglia in the rostral nucleus of the solitary tract and the active microglia may alter neuronal excitability of the NST neurons that process taste information conveyed by taste afferents resulting in

abnormal taste sensation.

As the first step to reveal a mechanism of abnormal taste sensation following IAN injury, this study investigated the appearance of microglia in the rNST in animal models of inferior alveolar nerve injury using an immunohistochemical approach in rats with inferior alveolar nerve transection as an IAN injury model.

MATERIALS AND METHODS

All experiments were conducted on 8 week old male Sprague-Dawley rats. The animals were housed on a 12-hour light cycle with access to standard food ad libitum. All protocols were approved by the Osaka Dental University Animal Research Committee (Approval numbers 12–03008, 13–04001 and 14–04005). For survival surgery, animals were anesthetized with intraperitoneal injections of sodium pentobarbital (50 mg/kg). The anesthetic level was assessed by lack of a reflex response to mild tail pinching. A small incision was made on the surface of the facial skin over the masseter muscle. The masseter muscle was dissected to expose the mandible. The IAN was exposed by removing mandibular bone, and transected at the angle of the mandible (IANx). The incision was closed with sutures. The animals were

moved to an isolated cage and when ambulatory, were returned to the dam's home cage.

After 1 day, 7 days and 3 weeks, the animals were given an overdose of sodium pentobarbital, and were euthanized by transcardiac fixative perfusion with 0.1 M phosphate buffered saline (PBS) followed by 4%
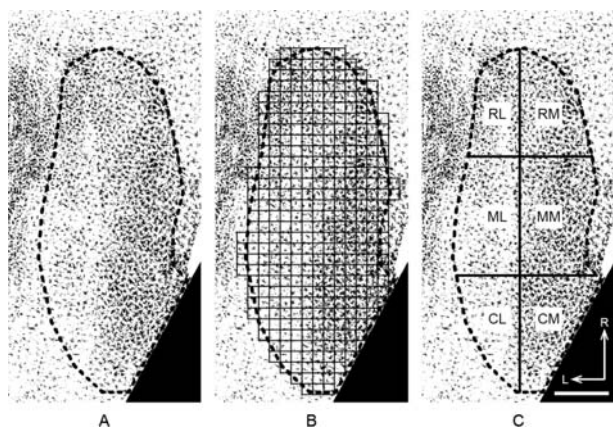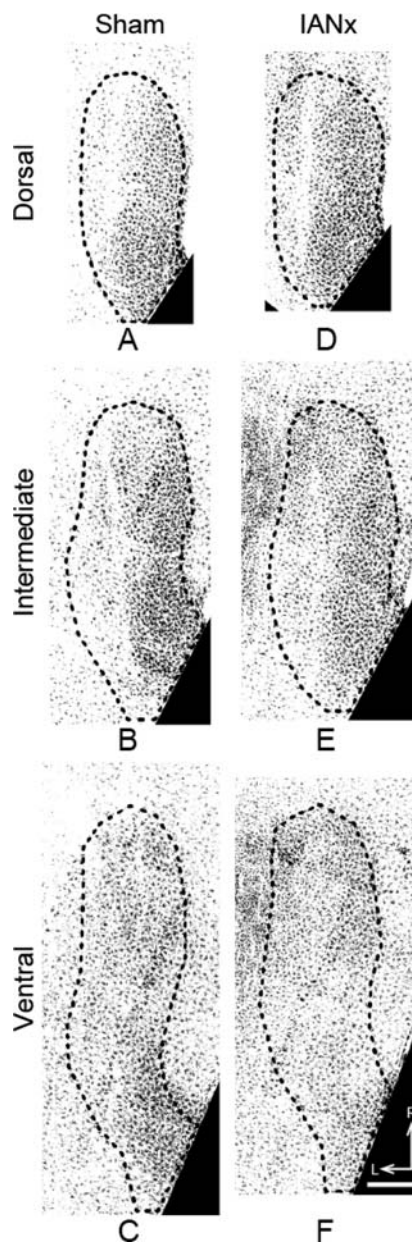

Fig. 2 Microglia at 7 days after surgery. Microglia are seen in horizontal sections from the NST after sham surgery (A–C) and after IANx (D–F). The dorsal (A and D), intermediate (B and E) and ventral (C and F) sections were from the dorsal third, middle third and ventral third of the NST, respectively. Bar : 0.5 mm.

Fig. 1 Method for quantifying density of Iba 1 labeling in the NST. (A) A binary image of pixels representing Iba 1 labeling in the NST is encircled with a dotted line. (B) The NST area was subdivided into 40×40 pixel grid boxes for pixel density analysis. (C) For statistical analysis, the NST area was divided into rostral-lateral (RL), rostral-medial (RM), middle-lateral (ML), middle-medial (MM), caudal-lateral (CL) and caudal-medial (CM) subfields.
R : Rostral, L : Lateral, Bar : 0.5 mm.

paraformaldehyde in 0.1 M PB of pH 7.4 at room temperature. The brains were postfixed overnight at 4°C in the same fixative. They were then blocked at the level of the pons just caudal to the obex, and sectioned horizontally into 50 μm-thick slices using a Vibratome (VT 1000 S ; Leica Microsystems Japan, Tokyo, Japan).

An anti-Iba 1 antibody (WAKO Pure Chemical Industries, Osaka, Japan) was diluted in PBS containing 1% normal goat serum, 1% bovine serum albumin, and 0.3% Triton X–100. They were then incubated overnight at 4°C. After washing the primary antibody, the tissue was incubated with Alexa Fluor 488 goat anti-rabbit IgG (H + L) antibody (Life technologies, Tokyo, Japan) for 2 hours at room temperature.

Iba 1(+) microglial cells were imaged using a laser scanning confocal microscope equipped with a 10 × objective (Leica Microsystems). Sequential optical sections were captured every 5 μm for each 50 μm section. A transmitted light image at 10 × was captured for every physical section. This permitted an accurate registration of common dorsal to ventral brainstem sections among the animals.

Quantification of Iba 1 was achieved using ImageJ software. To compare among sections, each image stack was initially rotated in ImageJ so that the solitary tract was oriented vertically. With the corresponding transmitted light image used as a reference, the border of the NST was outlined for each physical section. A threshold algorithm[1] was then applied to the
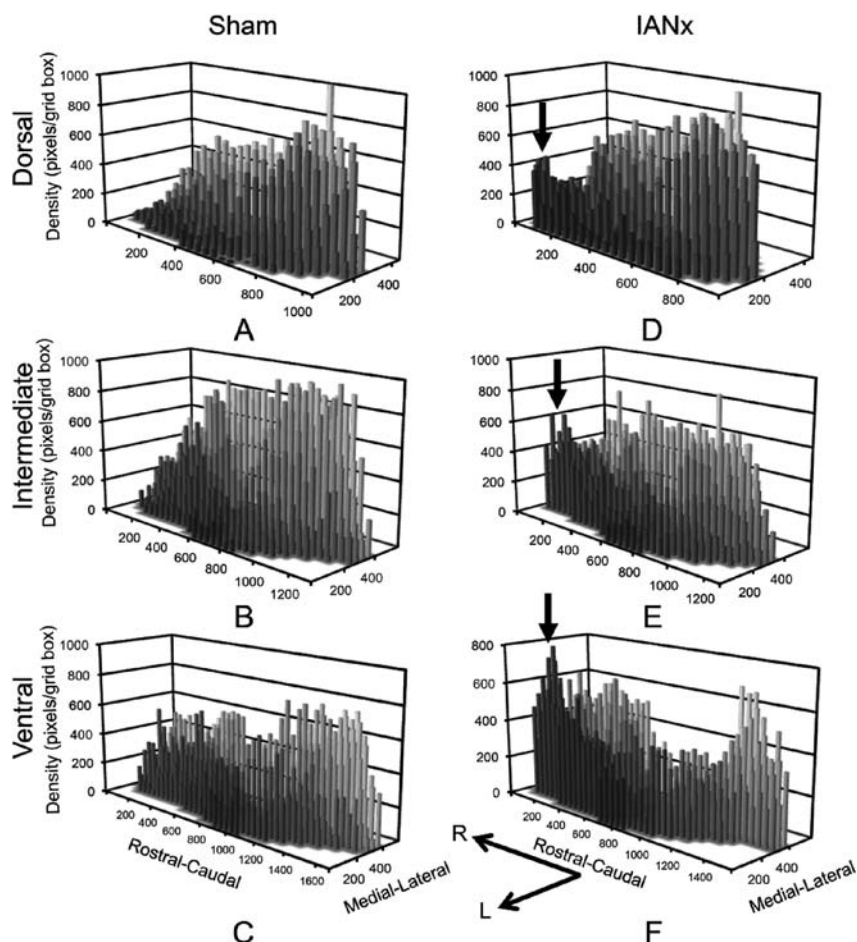

Fig. 3 Microglia densities at 7 days after surgery. This shows the density of Iba 1 labeling in the NST after sham surgery (A–C) and after IANx (D–F). The medial-lateral axis represents distance (μm) from the medial border of the NST, while the rostral-caudal axis represents the distance (μm) from the rostral pole of the NST. The z-axis ("density") represents the number of pixels with Iba 1 labeling in the 40 × 40 pixel grid boxes dividing the NST. See Materials and Methods for further detail.

entire image stack (Fig. 1 A). To identify where active microglia increased in number in the NST following the IANx procedure, the NST in the horizontal plane was subdivided into uniform grid boxes of 40×40 pixels ($100 \times 100 \ \mu$m) (Fig. 1 B). A particle analysis was performed to count the pixels above a threshold in each grid box by ImageJ. For statistical analysis, the pixel count was averaged for each subfield (Fig. 1 C).

Statistical analysis was conducted using EZR (Saitama Medical Center, Jichi Medical University, Saitama, Japan), which is a graphical user interface for R (The R Foundation for Statistical Computing, Vienna, Austria). More precisely, it is a modified version of the R commander designed to add statistical functions frequently used in biostatistics. The density of Iba 1 labeling was compared between the sham surgery animals and the IANx groups for each subfield using the Mann-Whitney U test with the significance level set at 0.05. The results are expressed as median and median absolute deviation.

RESULTS

At 7 days after sham surgery, the Iba 1(+) microglial cells were scattered throughout the NST, although not evenly distributed in the NST (Figs. 2 A–C). More Iba 1(+) microglial cells were seen in the caudal region of the NST (Figs. 2 A–C and 3 A–C). This trend was seen at all dorsal-ventral levels of the NST (Figs. 3 A–C).

After IAN damage in the mandibular duct, microglia reacted throughout the NST. At 1 day after injury, the microglia seemed more heavily stained with Iba 1, although the distribution of the cells appeared similar to the sham surgery case (Figs. 5 A and C). However, by 7 days post-IANx, a cluster of microglial cells appeared in and around the rostral-most portion of the NST (Figs. 2 D–F). In the NST, this microglial aggregate was mostly confined to the rostral-lateral portion and resulted in much denser and brighter Iba 1 staining in this portion (arrows in Figs. 3 D–F). To confirm the microglia aggregate in the rostral-lateral portion, the NST area was divided into a total of six subfields (Fig. 1 C) for statistical analysis. The density of Iba 1 labeling was significantly higher in the rostral-lateral
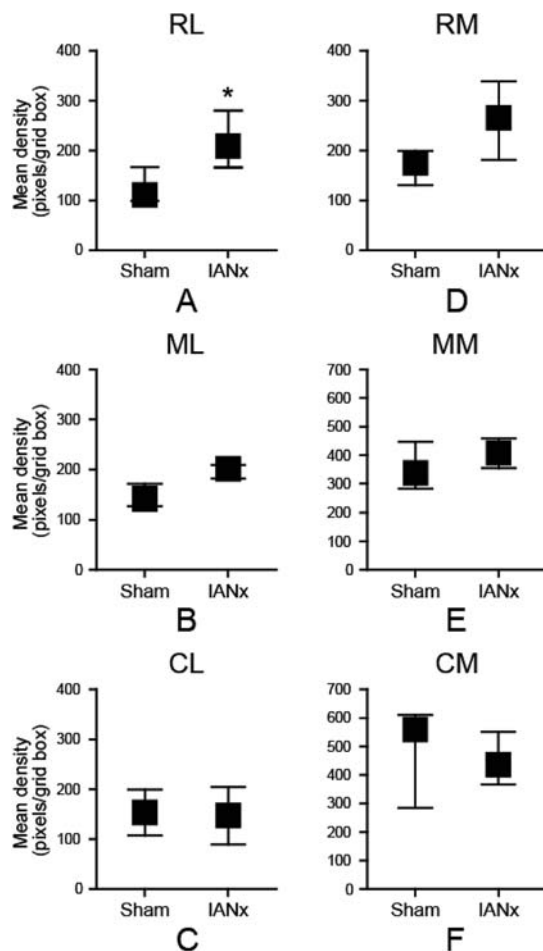

Fig. 4 Microglia densities in the subfields at 7 days after sham surgery compared with IANx. The "mean density" represents the mean number of the pixels with Iba 1 labeling in the 40×40 pixel grid boxes contained within the individual subfields in the middle third extent of the NST.

subfield at 7 days after IANx compared with sham surgery (Fig. 4 A), indicating that IANx induces the aggregation of microglia in the subfield. This clustering of cells and heavier Iba 1 staining disappeared by 3 weeks after injury (Fig. 5 D).

DISCUSSION

In the current study, peripheral transection of the IAN caused significant microglial responses in the first central gustatory relay, that is, NST. By 1 day after injury, many microglial cells appeared in the NST, the spinal trigeminal nucleus and the intermediate area of these nuclei. By 7 days after IANx, the number of microglial cells had increased significantly in the
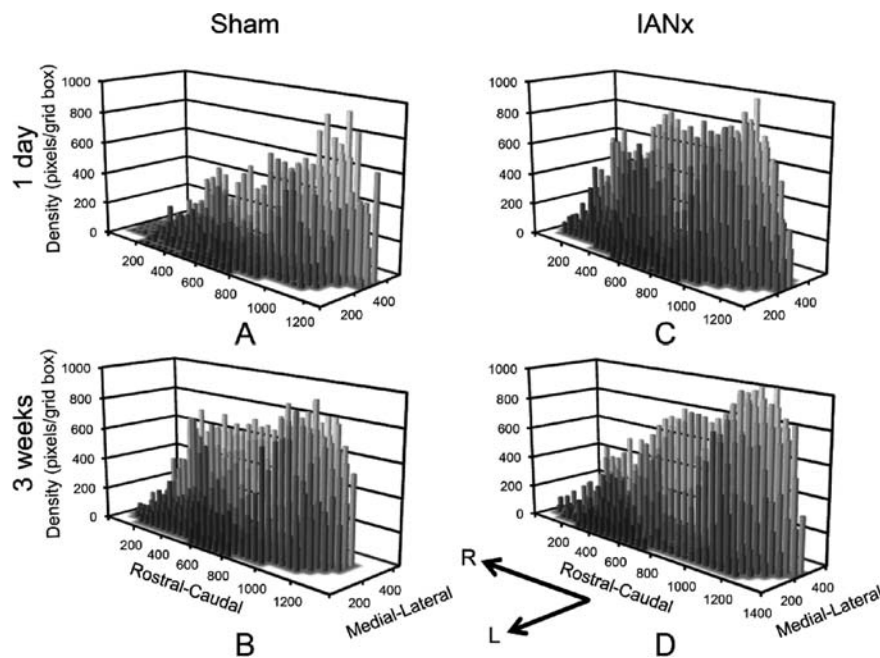
Fig. 5   Microglia densities in the middle third of the NST at 1 day (A and C) and 3 weeks (B and D) after surgery.

rostral-lateral portion of the NST. After that, the microglial numbers in this region slowly declined and returned to baseline by 3 weeks. Microglial cells quickly reacted with an increase in number after IAN damage. Although the signals mediating these microglial responses following nerve damage remain unclear, the pattern of responsive microglia in regions containing the central nerve terminals of the affected peripheral nerve suggests that the nerve fibers themselves are a source of signals activating microglial cells. There are reports on microglial response in central nerve terminals after injury of peripheral nerves innervating orofacial regions. For example, microglia react in the trigeminal sensory nuclear complex after IAN injury.[4, 10] In this study, microglial responses were seen in a limited area from the spinal trigeminal nucleus to the rostral-lateral portion of the NST, which receive afferent terminal projections from the IAN.[11] This spatial confinement strongly suggests that the signals leading to microglial responses are localized to the IAN afferent terminals.

The afferent branches of the facial nerve, chorda tympani and greater superficial petrosal nerves, are broadly considered to convey primarily taste informa-

tion.[12] Their most intense terminal fields are found in the rostrocentral subnucleus,[13] which contains neurons responding to taste stimuli applied to the oral cavity.[14–16] In addition, these nerves project in the rostrolateral subnucleus of the NST,[17–19] although the projections are sparse in comparison with their exceptional densities in the rostrocentral subnucleus, suggesting a strong contribution to sensory processing in the rostral-lateral subfield of the NST.

In the rostrolateral subnucleus of the NST, glossopharyngeal nerve projection is dominant to the chorda tympani and greater superficial petrosal nerve projections.[13] An anatomical study has reported that neurons in the rostrolateral subnucleus project to the forebrain and other brainstem locations.[20] Evidence derived from selective transection of the facial and glossopharyngeal nerves projecting in NST has demonstrated that facial nerve input is important in taste discrimination while glossopharyngeal input is related to reflex oral motor rejection circuits.[21] Thus neurons in the rostral-lateral subfield play important roles in sensory processing for both taste perception and taste-related behavior.

Reactive microglia can also contribute to neuronal

excitation by releasing substances that increase excitability or alleviate inhibition of neurons. For example, in animal models of chronic pain following peripheral nerve damage, reactive microglia in the first central relay nucleus of the affected nerve increase synthesis and secretion of various cytokines.[22, 23] These cytokines can then act on neurons in the relay nucleus to amplify neuronal excitation and sensory signaling.[22] In a similar fashion, the release of cytokines by reactive microglia may disturb neuronal activity in the NST, which underlies taste disorders such as higher threshold and lower intensity of taste following trigeminal deafferentation that result from tooth extraction and pulpectomy.[1, 3]

In summary, the current study revealed microglial responses in the rostral-lateral portion of the NST. This result could extend the involvement of the glial responses to include other sensory phenomena. As in the dorsal horn, in which reactive glia release substances that amplify neuronal excitation and pain signaling, a similar neuronal disturbance in the NST may underlie abnormal taste sensations following dental deafferentation.[1, 3]

REFERENCES

1. Shafer DM, Frank ME, Gent JF, Fischer ME. Gustatory function after third molar extraction. *Oral Surg Oral Med Oral Pathol Oral Radiol Endod* 1999 ; **87** : 419–428.
2. Hotta M, Endo S, Tomota H. Taste disturbance in two patients after dental anesthesia by inferior alveolar nerve block. *Acta Otolaryngol* 2002 ; **122** : 94–98.
3. Boucher Y, Berteretche MV, Farhang F, Arvy MP, Azérad J, Faurion A. Taste deficits related to dental deafferentation : an electrogustometric study in humans. *Eur J Oral Sci* 2006 ; **114** : 456–464.
4. Piao ZG, Cho IH, Park CK, Hong JP, Choi SY, Lee SJ, Lee S, Park K, Kim JS, Oh SB. Activation of glia and microglial p38 MAPK in medullary dorsal horn contributes to tactile hypersensitivity following trigeminal sensory nerve injury. *Pain* 2006 ; **121** : 219–231.
5. Hanisch UK. Microglia as a source and target of cytokines. *Glia* 2002 ; **40** : 140–155.
6. Watkins LR, Maier SF. Beyond neurons : evidence that immune and glial cells contribute to pathological pain states. *Physiol Rev* 2002 ; **82** : 981–1011.
7. Ledeboer A, Sloane EM, Milligan ED, Frank MG, Mahony JH, Maier SF, Watkins LR. Minocycline attenuates mechanical allodynia and proinflammatory cytokine expression in rat models of pain facilitation. *Pain* 2005 ; **115** : 71–83.
8. Braud A, Vandenbeuch A, Zerari-Mailly F, Boucher Y. Dental afferents project onto gustatory neurons in the nucleus of the solitary tract. *J Dent Res* 2012 ; **91** : 215–220.
9. Sahoo PK, Soltani S, Wong KC, Chen YC. A survey of thresholding techniques. *Comput Vis Graphics Image Process* 1988 ; **41** : 233–260.
10. Mostafeezur RM, Zakir HM, Yamada Y, Yamamura K, Iwata K, Sessle BJ, Kitagawa J. The effect of minocycline on the masticatory movements following the inferior alveolar nerve transection in freely moving rats. *Mol Pain* 2012 ; **8** : 27.
11. Takemura M, Sugimoto T, Sakai A. Topographic organization of central terminal region of different sensory branches of the rat mandibular nerve. *Exp Neurol* 1987 ; **96** : 540–557.
12. Whitehead MC, Finger TE. Gustatory pathways in fish and mammals. In : Firestein S, Beauchamp GK, editors. The senses : a comprehensive reference. Oxford, UK : Academic Press 2008 : 237–259.
13. Corson J, Aldridge A, Wilmoth K, Erisir A. A survey of oral cavity afferents to the rat nucleus tractus solitarii. *J Comp Neurol* 2012 ; **520** : 495–527.
14. McPheeters M, Hettinger TP, Nuding SC, Savoy LD, Whitehead MC, Frank ME. Taste-responsive neurons and their locations in the solitary nucleus of the hamster. *Neuroscience* 1990 ; **34** : 745–758.
15. Harrer MI, Travers SP. Topographic organization of Fos-like immunoreactivity in the rostral nucleus of the solitary tract evoked by gustatory stimulation with sucrose and quinine. *Brain Res* 1996 ; **711** : 125–137.
16. Travers SP, Hu H. Extranuclear projections of rNST neurons expressing gustatory-elicited Fos. *J Comp Neurol* 2000 ; **427** : 124–138.
17. Contreras RJ, Beckstead RM, Norgren R. The central projections of the trigeminal, facial, glossopharyngeal and vagus nerves : an autoradiographic study in the rat. *J Auton Nerv Syst* 1982 ; **6** : 303–322.
18. Whitehead MC, Frank ME. Anatomy of the gustatory system in the hamster : central projections of the chorda tympani and the lingual nerve. *J Comp Neurol* 1983 ; **220** : 378–395.
19. Whitehead MC. Neuronal architecture of the nucleus of the solitary tract in the hamster. *J Comp Neurol* 1988 ; **276** : 547 –572.
20. Halsell CB, Travers SP, Travers JB. Ascending and descending projections from the rostral nucleus of the solitary tract originate from separate neuronal populations. *Neuroscience* 1996 ; **72** : 185–197.
21. Spector AC, Travers SP. The representation of taste quality in the mammalian nervous system. *Behav Cogn Neurosci Rev* 2005 ; **4** : 143–191.
22. Zhuo M, Wu G, Wu LJ. Neuronal and microglial mechanisms of neuropathic pain. *Mol Brain* 2011 ; **4** : 31.
23. Daigo E, Sakuma Y, Miyoshi K, Noguchi K, Kotani J. Increased expression of interleukin-18 in the trigeminal spinal subnucleus caudalis after inferior alveolar nerve injury in the rat. *Neurosci Lett* 2012 ; **529** : 39–44.